Surface Science 605 (2011) 1480–1485

Contents lists available at ScienceDirect

Surface Science

journal homepage: www.elsevier.com/ locate/susc

The structure formed by the deposition of a sub-monolayer quantity of platinum onto Cu(110) investigated using medium energy ion scattering

T.P. Fleming [a], M.D. Cropper [a,*], P. Bailey [b], T.C.Q. Noakes [b]

[a] Department of Physics, Loughborough University, Loughborough, LE11 3TU, UK
[b] Daresbury Laboratory, Daresbury, Warrington, WA4 4AD, UK

ARTICLE INFO

Article history:
Received 21 March 2011
Accepted 13 May 2011
Available online 19 May 2011

Keywords:
Platinum Pt
Copper Cu(110)
Medium energy ion scattering (MEIS)
Pt/Cu surface alloy
Surface structure
Adsorption and deposition

ABSTRACT

The structure of 0.35 monolayers of platinum deposited onto Cu(110) has been investigated using medium energy ion scattering. Quantitative analysis of the data has been performed using the VEGAS routine. It was found that platinum atoms mostly occupy the second layer with a first interlayer distance of $d_{12} = 123 \pm 4$ pm and a separation of first and third layers of $d_{13} = 142^{+4}_{-10}$ pm. These represent a contraction of 4% and an expansion of 11% respectively from the ideal termination of the Cu(110) surface. There is clear evidence of the presence of some platinum in the third layer.

1. Introduction

The widespread interest in bimetallic surfaces and surface alloys has been motivated by the desire to understand the fundamental processes leading to surface alloying or to create model catalyst surfaces to investigate surface chemical reactions. One common theme has been the interaction of metals such as platinum or palladium with copper [1–3] and bulk alloys of these elements [4]. We present here an investigation of the structure formed by the interaction of sub-monolayer amounts of platinum with a non-close packed surface of fcc copper; the (110).

The interaction of platinum with low-index single-crystal copper surfaces has been the subject of several previous studies. The recurring theme of these has been the tendency to form a surface alloy between the deposit and the substrate, either at room temperature or elevated temperatures, presumably driven by the higher surface energy of platinum relative to copper [5,6]. On Cu(100) there is evidence of alloy formation, either at room temperature or following thermal activation, for sub-monolayer deposition. An ion scattering spectroscopy (ISS) study reported platinum film growth up to 3 ML but with copper atoms staying visible indicating a copper cap [7]. A subsequent low energy electron diffraction (LEED) investigation found an ordered second layer alloy following activation at 550 K [8]. Another investigation using low energy ion scattering (LEIS) [9] found intermixing of the platinum with the substrate surface that is enhanced by annealing to 573 K. A medium energy ion scattering (MEIS) investigation [10] of the interaction of platinum with Cu(111) found a surface alloy which involved platinum occupation of the first and second layers. This surface alloying occurred for deposition temperatures in the range 200 K to 450 K, but higher temperatures promoted diffusion into the third layer and beyond. It was found that deposition onto a vicinal surface promoted the occupation of the second layer by platinum, indicating that a step-mediated mechanism was involved.

Much less is known about the deposition of platinum onto the Cu(110) surface. Thermal energy atom scattering (TEAS) has been used [11] to investigate the effects of temperature on the behaviour of sub-monolayer amounts of platinum on the surface. For deposition of quite small amounts of platinum (<5% ML) at room temperature, the surface was found to be roughened, suggesting that platinum adatoms were present. For temperatures above 330 K, the surface was found to smoothen, indicating inclusion of the platinum within the surface.

Although there have been few reports on the behaviour of platinum on the Cu(110) surface a similar system, the deposition of palladium onto Cu(110), has been the subject of several investigations. This system has been studied primarily using scanning tunnelling microscopy (STM) [12–16] in combination with Auger electron microscopy (AES) [15], LEED [15,16], X-ray photoelectron spectroscopy [16] and reflection anisotropy spectroscopy [13]. There is also a report of an investigation using LEIS [17] which found that for deposition of 1 ML equivalent at room temperature only 15% of the palladium was visible in the surface layer, with copper atoms remaining visible. This supported the STM findings [12,15] that for deposition of sub-monolayer amounts, the palladium atoms displaced copper atoms in the surface layer to form a surface alloy. Substrate copper atoms were found to diffuse from the step edges to cover the palladium atoms [12] burying the palladium into

* Corresponding author. Tel.: +44 1509 223308; fax: +44 1509 223986.
E-mail address: m.d.cropper@lboro.ac.uk (M.D. Cropper).

0039-6028/$ – see front matter © 2011 Elsevier B.V. All rights reserved.
doi:10.1016/j.susc.2011.05.013

the second layer. Subsequent deposition formed a (2×1) superstructure with rows of alternating palladium and copper atoms aligned with the $[\bar{1}10]$ direction [12,15]. The STM images showed islands indicating the existence of a heterogeneous surface with areas of (2×1) and areas of clean copper. Post-deposition annealing (at relatively low temperatures) was found to smoothen the surface, as measured by STM [14], and to enhance intermixing [15].

The aim of the work reported here was to investigate the structure formed by the deposition of a sub-monolayer amount of platinum onto Cu(110). To do this we have employed MEIS, a refinement of Rutherford backscattering with enhanced surface sensitivity. Previously, MEIS has been shown to be a valuable technique for the investigation of metal-on-metal systems and surface alloying [10,18–21]. It may be used to determine surface structures by a shadowing and blocking approach, giving layer-by-layer composition [22] and structural parameters with high accuracy [23,24].

In this paper, we report the results of this MEIS investigation and show that when deposited onto the Cu(110) surface, platinum atoms displace copper surface atoms and preferentially occupy the second layer in the surface.

2. Experimental

All the experiments were performed at the UK National MEIS facility [25]. This apparatus comprises three principal sections connected by UHV transfer mechanisms and fast entry load lock. The ion source, accelerator and beamline produced a beam of H^+ ions of kinetic energy of 100 keV, energy resolution <0.1% and angular divergence <0.1°. The actual MEIS experiments take place in a scattering chamber equipped with a precision goniometer, which has three rotational and three translational axes, and a toroidal electrostatic ion analyser that disperses the scattered ions in energy whilst retaining their angular distribution for detection on a position sensitive detector. The sample cleaning, deposition, and initial characterisation take place in a typical surface science preparation chamber that is equipped with a sample stage that could be heated, low energy ion gun for crystal cleaning, deposition sources, a concentric hemispheres analyser for AES and a retarding field analyser for LEED.

During the experiments, the base pressure of the preparation chamber was 8×10^{-10} mbar. The Cu(110) crystal supplied by Surface Preparation Laboratory, The Netherlands had been aligned to better than 0.5° and was cleaned by repeated cycles of sputtering using 1.5 keV Ar^+ ions followed by annealing to 773 K. After several cycles, a clean and ordered surface was produced as determined by AES and observation of the LEED pattern. Platinum was deposited onto the clean surface at 330 K using a water-cooled miniature e-beam evaporator (EBE-1, Oxford Instruments) loaded with a 1 mm platinum feedstock of purity 99.99% (Advent Research Materials). During deposition the chamber pressure was kept below 10^{-8} mbar. The platinum dose was determined using MEIS in a non-aligned "random" direction, and confirmed using the aligned spectra once suitable models had been constructed.

The MEIS measurements utilised three different incident alignments, with the beam anti-parallel to each of the [101], [100] and [121] directions (illustrated in Fig. 1). Two of these geometries utilised scattering in the plane defined by the surface normal and the $[\bar{1}1\bar{2}]$ azimuthal direction. The $[\bar{1}0\bar{1}]$ geometry has a nominal one-layer illumination, with surface layer atoms partially shadowing atoms in the second and deeper layers. There is sufficient illumination of the second layer (due to thermal vibrations of the first layer) to produce a blocking dip which corresponds to the $[01\bar{1}]$ direction. The $[\bar{1}2\bar{1}]$ geometry illuminates fully the top three layers and over the range of scattering angles used gives several blocking dips that are sensitive to occupation of layers two to four. The final incident geometry involved scattering in a different plane, that defined by the surface normal and the $[\bar{1}10]$ direction. Incidence in the $[\bar{1}00]$ direction illuminates fully the top two layers, but involves two inequivalent scattering planes; one containing the surface "row" atoms and one containing the surface "trough" atoms, illustrated in Fig. 1(a).

As is usual for this facility, the data were collected in the form of two dimensional tiles which display counts versus scattering angle and ion energy. The large mass difference of the two elements involved meant that the blocking curves originating in scattering from both elements could be separated in a straight forward manner, except for the low scattering angles used in the $[\bar{1}0\bar{1}]$ geometry where extracted yields will be less reliable. The scattering angles of the surface blocking-curves were calibrated by comparison of the deep bulk blocking curves with simulations for a perfect Cu(110) crystal.

The quantitative surface structural determination was performed by simulation using the VEGAS routine developed at FOM [26] and combined with a user-friendly interface developed at the University of Warwick [27]. The data that are presented have been corrected for the Rutherford scattering cross-section and then calibrated into units of visible monolayers. The basis of this calibration was to use data extracted for the clean Cu(110) surface and to compare it with simulations made using the parameters determined in a previously published MEIS investigation [28]. The blocking curves produced using the MEIS facility are known to have small tilts on them due to the variation in sensitivity of the detector across the angular range. For this reason, where simulations have been compared with data they have had small count-conserving linear corrections applied to them and limited scaling has been allowed within the constraints of the generally accepted accuracy of the procedure that extracts visible monolayers.

3. Results and discussion

The data collected following deposition of platinum at 330 K are shown in Fig. 2. The blocking curve formed by scattering from the platinum is indicated by filled circles and that from the copper by open circles. The solid lines are the result of modelling, which will be discussed later. The ion scattering yield from the platinum indicates that the amount of platinum deposited was equivalent to 0.35 ML where a monolayer is defined in terms of the single layer atomic density of copper in the Cu(110) surface (1.08×10^{19} m^{-2}). Several notable features are immediately apparent from the data, the main one being that the platinum blocking curves exhibit dips indicating that significant amounts of platinum are located below the surface layer.

The visibilities of the curves in Fig. 2 deserve some comment. As stated previously, the geometries correspond to nominal one-, two- and three-layer alignments. For a perfect crystal with no thermal vibrations, the total visibilities of copper and palladium combined in these curves would be one, two and three ML. However, static imperfections such as surface relaxations and dynamic imperfections such as thermal vibrations, particularly surface-enhanced vibrations, result in subsurface atoms being imperfectly shadowed, increasing the total visibility. So, although the second layer in principle should be completely shadowed in the one-layer alignment, in practice more than half of the second layer contributes to the scattering. This is particularly important for the platinum blocking curve, which will be discussed later. Indeed the number of visible layers in each scattering geometry can make an important contribution to the surface structural determination as it is affected by surface relaxations.

The one layer alignment (Fig. 2(a)) shows a dip near 60° scattering angle in the copper blocking curve that is due to a one-layer outgoing event illustrated in Fig. 1(b). This dip is replicated in the platinum blocking curve indicating platinum atoms are in a sub-surface layer. The relatively high visibility of this blocking curve suggests that this is mainly in the second layer; if large amounts of the platinum were in lower layers it would be very effectively shadowed, but shadowing is not perfect in the second layer as mentioned above. Further inspection

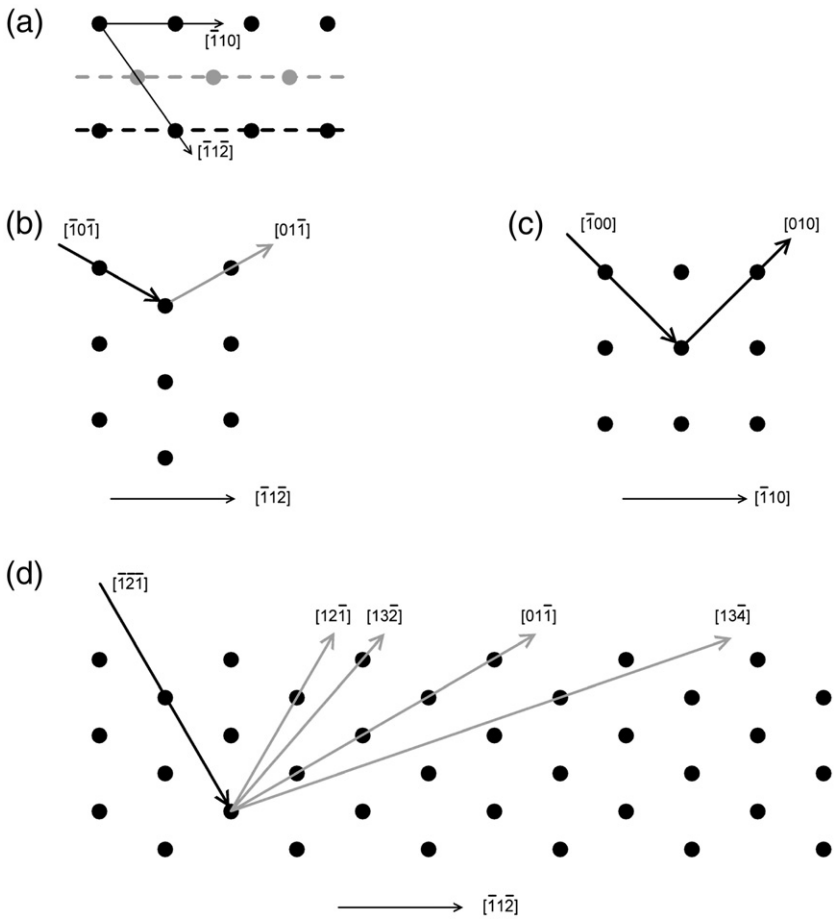

Fig. 1. The medium energy ion scattering geometries employed and some of the principal blocking events. A plan schematic of the surface is shown in (a) with both scattering planes indicated (row atoms are black circles and trough atoms are grey circles). Cross sections of the scattering planes are shown in (b), (c) and (d). Note that for the [1̄00] geometry, (c), there are two different but similar scattering planes indicated by the black and grey circles in (a).

of this blocking dip shows that it is shifted to lower scattering angle than the nominal 60° expected for a perfect fcc lattice. This indicates that the interlayer distance between the second layer platinum and the top layer is reduced compared with a simple Cu(110) termination. A similar contraction has been reported for clean Cu(110) [28].

Moving to the two layer illumination (Fig. 2(b)) the dip near 90° in the copper blocking curve is due to the [010] outgoing direction; first appearing in scattering from the third layer. This dip is not strongly evident in the platinum curve and the complete illumination of the platinum in this geometry confirms the conclusion that the majority of the platinum atoms are located in the top two layers.

The three layer illumination (Fig. 2(c)) contains several pieces of information. The copper blocking curve has four main dips. The one near 90° nominal scattering angle results from a one-layer (110) type event, that near 76.1° requires occupation of the third layer and that near 120° occupation of the fourth. In the platinum blocking curve the one-layer dip is strongly present, which is consistent with the dip in the one-layer illumination. In addition there is evidence of a dip near 76.1° suggesting some platinum is located in the third layer (the data are shown enlarged in the inset to Fig. 2(c)). However, there is no clear cut evidence for occupation of the fourth layer, which would put a dip near 120°. Platinum occupation of the third layer would be expected to put a dip near 90° in the [1̄00] data; this is possibly just visible as shown in the inset to Fig. 2(b).

Further evidence about the layer-by-layer composition can be obtained by comparing the relative visibilities of the platinum in the three incident geometries. The platinum is fully, or close to fully visible for the [1̄00] two-layer and [1̄2̄1̄] three-layer geometry, but is slightly reduced to around 0.28 for the [1̄0̄1̄] one-layer geometry. This is due to shadowing of platinum atoms in the second layer, by first layer atoms. The precise quantification of this effect requires a full simulation as the effectiveness of shadowing is influenced by parameters other than layer-by-layer composition, such as the interlayer distances and the thermal vibrations. That the clear presence of platinum in the second layer is due to simple islanding in an overlayer film can be eliminated by a combination of the relative visibilities of copper and platinum and the depth of the platinum blocking dips, as was found in the results of quantitative modelling discussed below.

The mechanism for the incorporation of the platinum atoms into the second and even third layers requires comment. This is unlikely to occur by bulk diffusion at these low temperatures so a surface diffusion mechanism is more likely. It is known that atoms on the Cu (110) surface are mobile at room temperature [29] and the incorporation of the platinum atoms into the surface layer could occur either by occupation of a vacancy left by a migrating copper atom or, more likely, by a direct displacement of a surface layer atom. Field ion microscope observations of the behaviour of platinum on a Ni(110) surface [30] favours the latter. In this work, platinum atoms were observed to displace surface nickel atoms by a concerted action of the two atoms displacing along the [1̄1̄2̄] azimuthal direction, illustrated in Fig. 3. This leaves platinum incorporated into the surface layer and a displaced surface atom in a new layer above. The

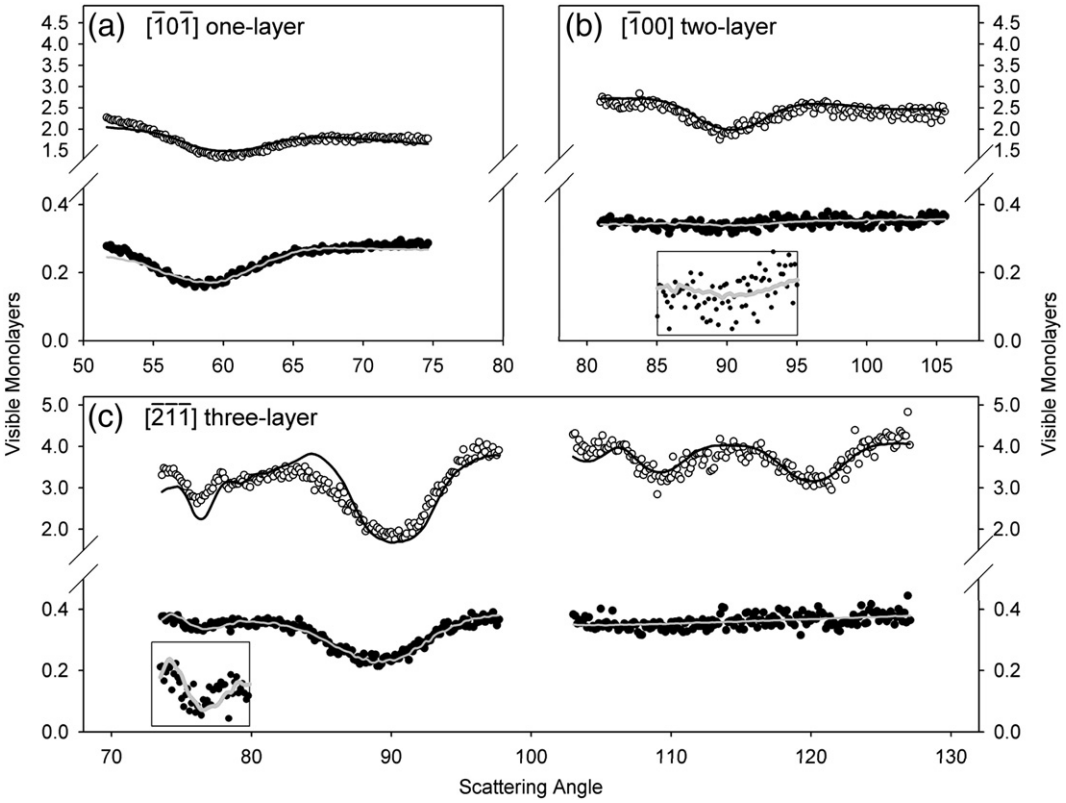

Fig. 2. Medium energy ion scattering blocking curves from the surface structure formed by the deposition of 0.35 monolayers of platinum onto Cu(110) at 330 K. The figure shows the copper (open circles) and platinum (filled circles) blocking curves for (a) [$\bar{1}0\bar{1}$], (b) [$\bar{1}00$] and (c) [$\bar{2}\bar{1}\bar{1}$] incidence directions. The solid lines are the results of simulations discussed in the text.

completion of this new surface layer and, indeed, the formation in some locations of another new layer above this is likely to happen by migration of copper atoms from step edges as is the case with the palladium on Cu(110), a system that has been studied by STM [12].

The key parameters that may be determined using MEIS are interlayer distances. Although these influence the visibility of lower layers, the main impact they have on the blocking curve is in the position of the dips. For the data presented here, the first interlayer distance is most sensitively revealed by the dips in the platinum blocking curves corresponding to the [$01\bar{1}$] nearest neighbour outgoing blocking event. For the data collected in the [$\bar{1}0\bar{1}$] incident geometry this dip would be at 60° for an ideal fcc crystal and for the data from the [$\bar{2}\bar{1}\bar{1}$] geometry the same dip would be at 90°. As has been mentioned, inspection of Fig. 2 indicates that the dip is shifted to lower scattering angle in both geometries revealing an interlayer distance that is contracted relative to bulk copper. A complication is that the dip in the [$\bar{1}0\bar{1}$] blocking curve is dominated by the first interlayer distance whereas the same dip in the [$\bar{2}\bar{1}\bar{1}$] is influenced by any platinum that is in the third or lower layers. Slight differences between geometries in the size of the shift of this dip in the platinum blocking curve from the expected ideal angle is further evidence that there is some platinum occupation of the third layer.

To obtain quantitative information about the surface structure, modelling of the blocking curves was carried out using the VEGAS simulation code [26]. The aim of this modelling was to determine the interlayer distances and the layer-by-layer composition. The approach taken in determining the layer-by-layer composition was to build models with platinum confined to each of the top four layers and to combine these linearly and then to optimise the fit to the data by varying the coefficients. One issue to be considered was the fractional monolayer of platinum present. Comparison with the structure of Pd on Cu(110) [12,15] suggests an appropriate model would be one with domains of approximately 50% platinum occupation that is complemented by domains that are entirely clean Cu(110). The results of the optimisation procedure were actually found to be quite insensitive to the relative weight given to these two domains and to the precise detail of the model, particularly in the fitting of the platinum blocking curve.

The parameters that were optimised in this way using the VEGAS model were the layer-by-layer occupation of platinum, interlayer distances and the thermal vibrations. In the domains where layers included both platinum and copper atoms, the interlayer distances were varied independently; that is the effect of surface corrugation was investigated. The accuracy of the structural parameters determined from these models was estimated using the Rχ method,

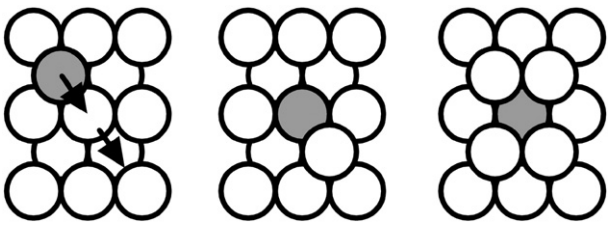

Fig. 3. A schematic of a possible mechanism for the incorporation of platinum into the second layer. A platinum atom deposited onto the surface displaces a copper atom into the top layer along the [$\bar{1}1\bar{2}$] azimuthal direction. Subsequent diffusion from step edges completes the copper overlayer.

frequently employed in MEIS [23]. In this method, the true chi-squared reliability factor is defined as

$$R_\chi = \frac{1}{n}\sum_{1}^{n}\frac{(I_{exp}-\lambda I_{sim})^2}{I_{exp}} \quad (1)$$

where I_{exp} is the non-Rutherford corrected counts in the surface peak, I_{sim} is the output from a VEGAS simulation in monolayers that has been modified by the Rutherford cross-section, λ is a scaling factor determined from the calibration from a clean Cu(110) surface but that is allowed to optimise within the constraints of $\pm 10\%$, and the summation is across all the n angular data points. In this case, where we have three datasets the actual R_χ used is a combination of the individual R_χ from each dataset weighted by the number of data points. The variation of R_χ with a particular parameter around its optimised value enables the estimation of the precision in determination of the parameter. For non-correlated parameters, the standard error σ_z in an optimised parameter, z_o is given by

$$\sigma_z^2 = \frac{2}{\left(\frac{\partial^2 R_\chi}{\partial z^2}\right)_{Z_o}}. \quad (2)$$

The solid lines superimposed on the data in Fig. 2 are the results of simulations using these optimised models. It was found that the quantitative analysis supported the initial conclusion that the platinum was mostly to be found in the second layer: putting most of the platinum in the top layer was inconsistent with the depth of the blocking dips and the relative visibility of the platinum in the three geometries for all of the physically acceptable ranges of the structural and non-structural parameters such as interlayer distance and thermal vibrations. The simulations shown in Fig. 2 are based on a first layer occupation of 0.03 ML, second layer of 0.29 ML and third (and possibly subsequent) layers 0.03 ML. The qualifying statement on this last figure reflects the lack of precision in the simulations in distinguishing between the third and fourth layers as these are equivalent in the [$\bar{1}$00] geometry and make contributions to the data collected in the [$\bar{1}2\bar{1}$] geometry that are not very different. The accuracy in these determinations is about 0.03 ML in each, indicating that only the platinum content of the second layer may be determined with precision. Fig. 4(a) and (b) show Rχ contour plots for the amount of platinum in the second layer against the other two layers. It is clear from these that the platinum is predominantly in the second layer.

These simulations also yielded information on the thermal vibration of the surface atoms. The main influence of these vibrations on the simulations is in the depth of the blocking dips and the visibility of lower layers that are notionally blocked in an ideal crystal. Optimising the model structure against these quantities, it was found that inclusion of platinum into the surface reduced the thermal vibrations of the second layer compared with those reported for clean copper [28] in a manner consistent with the larger mass of platinum atoms. We determined the mean square displacement of the platinum atoms to be 8 pm and that of the top layer copper atoms to be 11 pm (similar to that from reference [28]). The vibration of subsequent layers was indistinguishable from that of bulk copper (around 7 pm).

The final piece of information to be obtained from the simulations was the interlayer distances. The first interlayer distance for platinum (that is the distance between the top layer copper atoms and second layer platinum atoms) was determined to be $d_{12} = 123$ pm. This distance is a 4% contraction from that for bulk copper (110) planes

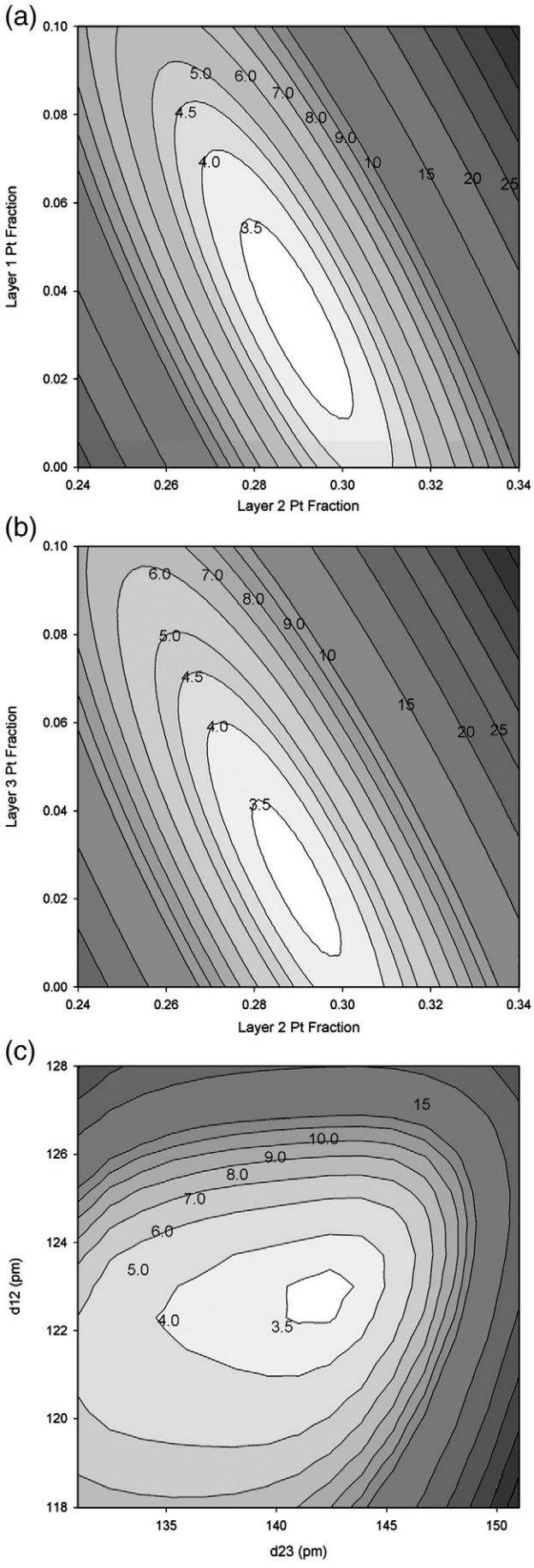

Fig. 4. Rχ contour plots for (a) the fractions of platinum in the first and second layers, (b) the fractions of platinum in the second and third layers, and (c) the two interlayer distances d_{12} and d_{23}.

(127.8 pm) but a 4% expansion over the reported first interlayer distance of clean Cu(110) which is 118 ± 2 pm [28], the expansion being consistent with the larger radius of platinum. The first interlayer distance for copper to copper could not be determined sufficiently accurately to enable an error to be estimated, but the simulations optimised at around 135 pm. That is there may be surface rumpling present, but the statistics did not allow precise determination of this. The position of the third layer distance influences the dips near 74° and 90° in the data collected in the [$\bar{2}\bar{1}\bar{1}$] incidence geometry. The second interlayer distance was found to be $d_{23} = 142$ pm, an expansion of 11% over the bulk copper inter-plane distance, but this figure is influenced by both the platinum and non-platinum containing sites. A formal error analysis of these two interlayer distances was carried out. The uncertainty in d_{12} was found to be 4 pm including the effect of the correlation between d_{12} and d_{23} shown in Fig. 4(c). The minimum in $R\chi$ for d_{23} is asymmetric, complicating the estimate of accuracy. Fitting separate functions to each side of the minimum yielded uncertainties of +4 pm and −10 pm.

The quantitative analysis of the data has revealed two specific aspects; that the highest concentration of platinum is to be found in the second layer and that the platinum induces a small expansion of the first interlayer distance. These results are consistent with literature reports on similar systems. The incorporation of platinum into the Cu(110) surface was seen in the TEAS work [11] and has been reported for the (111) [10] and (100) [9] surfaces. An ion scattering investigation of the (111) surface of the bulk Cu_3Pt alloy [31] found a second layer enrichment of platinum which was thought to be driven by the lower heat of vaporisation of Cu in competition with strain energy induced by the larger size of the platinum atoms. A similar element, palladium, has been shown [12] to incorporate into the second layer of both Cu(110) and Ag(110), together with the observation using STM of etch pits caused by copper or silver migrating to cap the palladium alloy layer. The expansion of the top layer due to the inclusion of the larger platinum atoms is to be expected, but is slightly smaller than the expansion observed for the incorporation of platinum into the Ni(110) surface [32].

4. Summary

Using the double-alignment method in MEIS we have shown that when it is deposited onto Cu(110) at 330 K platinum preferentially occupies the second layer. There is also clear evidence of some occupation of the third layer. The first interlayer distance is $d_{12} = 123 \pm 4$ pm and the separation of second and third layers is $d_{23} = 142^{+4}_{-10}$ pm. These respectively represent a contraction of 4% and an expansion of 11% over the bulk copper (110) distance, but the former is a 4% expansion over the reported Cu(110) surface interlayer distance [28]. The thermal vibrations of the surface layers were found to be 11 pm for the outermost copper atoms and 8 pm for the platinum atoms in the second layer.

Acknowledgments

We would like to thank the EPSRC for facility access under EP/E003370/1 and for a studentship for TPF. We would also like to thank the FOM for access to the VEGAS code, Paul Quinn for the interface and Paul Whitfield for technical support during the experiments.

References

[1] T. Wadayama, H. Osano, H. Yoshida, S. Oda, N. Todoroki, Applied Surface Science 254 (2008) 5380.
[2] L. Constant, P. Ruiz, M. Abel, Y. Robach, L. Porte, J.C. Bertolini, Topics in Catalysis 14 (2001) 125.
[3] B. Schaefer, M. Nohlen, K. Wandelt, The Journal of Physical Chemistry B 108 (2004) 14663.
[4] Y.G. Shen, D.J. O'Connor, R.J. MacDonald, Australian Journal of Physics 49 (1996) 689.
[5] A. Christensen, A.V. Ruban, P. Stoltze, K.W. Jacobsen, H.L. Skriver, J.K. Norskov, F. Besenbacher, Physical Review B 56 (1997) 5822.
[6] M. Schurmans, J. Luyten, C. Creemers, R. Declerck, M. Waroquier, Physical Review B 76 (2007).
[7] G.W. Graham, P.J. Schmitz, P.A. Thiel, Physical Review B 41 (1990) 3353.
[8] E. AlShamaileh, H. Younis, C.J. Barnes, K. Pussi, M. Lindroos, Surface Science 515 (2002) 94.
[9] M. Walker, C.R. Parkinson, M. Draxler, C.F. McConville, Surface Science 584 (2005) 153.
[10] P.C. Dastoor, D.J. O'Connor, D.A. MacLaren, W. Allison, T.C.Q. Noakes, P. Bailey, Surface Science 588 (2005) 101.
[11] M.B. Hugenschmidt, C. de Beauvais, Surface Science 307–309 (1994) 455.
[12] P.W. Murray, S. Thorshaug, I. Stensgaard, F. Besenbacher, E. Laegsgaard, A.V. Ruban, K.W. Jacobsen, G. Kopidakis, H.L. Skriver, Physical Review B 55 (1997) 1380.
[13] N.P. Blanchard, D.S. Martin, A.M. Davarpanah, S.D. Barrett, P. Weightman, Physica Status Solidi A-Applied Research 188 (2001) 1505.
[14] M. Abel, Y. Robach, L. Porte, Surface Science 498 (2002) 244.
[15] R.A. Bennett, S. Poulston, N.J. Price, J.P. Reilly, C.J. Barnes, M. Bowker, Surface Science 433 (1999) 816.
[16] J.P. Reilly, C.J. Barnes, N.J. Price, R.A. Bennett, S. Poulston, P. Stone, M. Bowker, Journal of Physical Chemistry B 103 (1999) 6521.
[17] P. Delichere, J.C. Bertolini, Surface and Interface Analysis 34 (2002) 116.
[18] C.J. Howe, M.D. Cropper, T.P. Fleming, R.M. Wardle, P. Bailey, T.C.Q. Noakes, Surface Science 604 (2010) 201.
[19] M.T. Butterfield, M.D. Crapper, T.C.Q. Noakes, P. Bailey, G.J. Jackson, D.P. Woodruff, Physical Review B 62 (2000) 16984.
[20] M.D. Cropper, T.C.Q. Noakes, M.T. Butterfield, P. Bailey, Surface Science 594 (2005) 212.
[21] T.C.Q. Noakes, P. Bailey, D.T. Dekadjevi, M.A. Howson, Physical Review B 68 (2003) 097335.
[22] P. Bailey, T.C.Q. Noakes, C.J. Baddeley, G. van der Laan, D. Brown, P.D. Quinn, D.P. Woodruff, Current Applied Physics 3 (2003) 89.
[23] D. Brown, T.C.Q. Noakes, D.P. Woodruff, P. Bailey, Y. Le Goaziou, Journal of Physics-Condensed Matter 11 (1999) 1889.
[24] T.J. Wood, C. Bonet, T.C.Q. Noakes, P. Bailey, S.P. Tear, Surface Science 598 (2005) 120.
[25] P. Bailey, T.C.Q. Noakes, D.P. Woodruff, Surface Science 426 (1999) 358.
[26] R.M. Tromp, J.F. van der Veen, Surface Science 133 (1983) 159.
[27] XVegas, Version 132, Paul Quinn, , 2005.
[28] M. Copel, T. Gustafsson, W.R. Graham, S.M. Yalisove, Physical Review B 33 (1986) 8110.
[29] Y.N. Wen, J.M. Zhang, K.W. Xu, Applied Surface Science 256 (2009) 1521.
[30] G.L. Kellogg, Physical Review Letters 67 (1991) 216.
[31] Y.G. Shen, D.J. O'Connor, K. Wandelt, R.J. MacDonald, Surface Science 328 (1995) 21.
[32] M. Walker, C.R. Parkinson, M. Draxler, C.F. McConville, Nuclear Instruments and Methods in Physics Research B249 (2006) 314.